Journal of Applied Sciences and Nanotechnology

Room Temperature 2-Fold Morphology Porous Silicon Impedance Matching Pesticide Sensor

[1]Rasha B. Rashid, [1]Alwan M. Alwan*, [1]Mohammed S. Mohammed

[1]Department of Applied Sciences, University of Technology – Iraq

A R T I C L E   I N F O

Corresponding Author:
Alwan M. Alwan
alkrzsm@yahoo.com

A B S T R A C T

In this work, an investigation was conducted to study the effect of electrodes' configuration of the double morphology macPSi on the performance of electrically matched impedance pesticides sensors. The purpose was to develop an efficient electrical sensor for the quantitative detection process of (Chlorpyrifos) pesticide in organic solvents. The effect of electrodes configuration of the front, front-back, and back coplanar electrodes on macPSi as based substrate was tested to select an optimum sensor metallization pathway. The based efficient macPSi layer was fabricated using elevated laser irradiation power density at different periods. Morphological, optical, and electrical properties of the sensors were investigated using field emission scanning electron microscope (FE-SEM), X-ray diffraction (XRD), photoluminescence (PL) spectroscopy, and R-L-C measurement. The sensing method depended on measuring the resonance frequency shift as the organic solvent was exposed to the sensor's surface. The sensor's performance at various configurations and concentrations ppm was inspected at room temperature. The current findings revealed extremely low instabilities (less than 0.017 %), higher sensitivity, and a detection limit of 0.004ppm for top coplanar electrode configuration. The fabricated sensor is simple and low-cost for excellent quantitative pesticide detection.

1. Introduction

Organic vapors and pesticides (such as methanol, acetone, and chlorpyrifos) are very dangerous for humans. They could hit the respiratory system if a person inhales a high dose of these vapors or pesticides. A healthy human has a low concentration of organic vapor or pesticides in his breath or food, while a high concentration indicates the presence of a disease. Nowadays, it is important to construct a highly sensitive and selective chemical sensor for food safety, industrial processes monitoring, healthcare, and atmospheric protection [1, 2]. Therefore, it is important to design a sensor with high sensitivity, stability, low detection limit, and working under ambient conditions. Porous silicon (PSi) and its different morphologies (pores, trenches, muds, and pillars like structures) provide a convenient, simple, and low-cost chemical sensor for the specifying pesticide content in its organic solution at very low concentration due to its high specific surface area and high reactivity [3]. PSi is an ideal-based material for sensors of liquids [4], either with Plasmonics material as in surface-enhanced Raman scattering optical sensors or capacitive sensors with pores or mud-like structures [5-7]. The basic principle advantage of the PSi

layers is attributed to their changeable properties; depending on the substance inside the porous matrix [8-10]. These features will help the PSi to be very suitable for optical and electrical sensing detection applications such as PSi /metallic nanoparticles SERS detection, humidity sensing, optoelectronic sensing of toxic gas detection, and pesticide detection in agriculture products [11-13]. The PSi optical sensors; working in a hazardous environment, provide the fastest read output, while conventional sensing equipment is so costly and suffers from environmental interference. The synthesis of PSi with different morphologies like pores, pillars, and trenches structures was carried out via several etching methods like electrochemical, stain, and photo-electrochemical etching processes [14-16]. Among those, the method photo-electrochemical is low cost, well-controlled, and has an efficient pathway for preparing specific surface morphologies by controlling laser power density and irradiation period during the etching cycle [17]. The adsorption rate of chemical species on the PSi surface varies according to the morphology type. Higher adsorption rate and hence detection of very low chemical species concentration can be achieved with a double macro PSi layer; due to the large specific surface area and reactivity [18]. The combination of various Psi morphologies in the porous matrix has a very important role in the PSi sensitivity; due to the Schottky-like junction formation and the impedance of fabricated sensors [19]. The current work aims to synthesize and develop an efficient impedance matching electrical sensor by employing double-layer macPSi with mud-like and pore-like morphologies using the photo-electrochemical etching pathway.

2. Experimental Procedure

The 2-fold morphology macPSi layer was synthesized through the etching of donor-type (100) silicon substrate of (0.1 Ω.cm) resistivity in 16 % HF concentration, (1:3) electrolyte solution (HF 48%: C_2H_5OH 99.99%) as shown in Fig. 1. The macPSi was formed via graded laser irradiation power density at multiple times of a constant etching period of 10 min. The graded photo-electrochemical process was carried out using 90 mW/cm^2 laser power density using 530nm diode laser wavelength at multiple times of 4-min period using 90 mW/cm^2 laser power density and 3min for both 60 and 30 mW/cm^2 laser power density. The etching current density was decreased from 60m/cm^2 to 20mA/cm^2 at three steps during the graded etching pathway. The macPSi formation was conducted at room temperature and involved a two-electrode configuration in which the Si substrate acts as an anode and a platinum ring as the cathode. The laser beam was defocused to satisfy a circular irradiation area of about 2 cm^2. Both the porosity and the layer thickness of the macPSi were calculated gravimetrically. The morphological properties of macPSi were carried out by VEGA TESCAN- 3SB Field Emission - scanning electron microscope (FE-SEM), and XRD-6000, Shimadzu X-ray diffract meter was calculated in the (Razi metallurgical research center – Iran), while the photoluminescence PL spectrum was measured using Jobin-Yvon T64000 with CW 323 nm, 300 mW - He-Cd laser The SEM was calculation in the ministry of science and technology-Iraq. The current-frequency characteristics were inspected by evaporating an Ohmic contact Aluminum electrode with three different configurations. The position and configuration of the electrodes are crucial in the value of macPSi layer capacitance; the sensitivity of the fabricated sensors. The three different forms of the fabricated capacitive macPSi sensors: coplanar back electrode (S1), front-back electrode (S2), and coplanar front electrode (S3) on the macPSi are illustrated in Fig. 2. For electrical contacts in the fabricated sensors, two copper wires were bonded to the macPSi using silver (Ag) paste. In the case of the vapors sensing process, the vaporized gas from diluted organic solutions (methanol and acetone) was warmed up by a heater and introduced through a tube into the sensing chamber by a stream of N_2 gas which acts as a carrier gas. Each read-out was performed after 50 sec of exposure time to the gas. The resonance frequency measurement in the impedance matching circuit was carried out using hp33120a high precision function generator and 8846AFluke 6-1/2 Digit precision multimeter. The sensitivity S% is given by the ratio between the resonance frequency shift Δf before and after exposure, to the frequency before the exposure, as shown in Eq. (1) [20].

$$S\% = \Delta f / f_o \tag{1}$$

The ability of a sensor to detect the smallest concentration of target molecules is called the limit of detection and is given as Eq. (2) [21].

$$LOD = 3SD/slope \tag{2}$$

Where; SD is the standard deviation, and the slope is taken from the plot between sensitivity and the target concentration. The simple impedance matching electrical circuit consists of an external coil, capacitive macPSi sensor, and a function generator with frequency ranging from 1KHz to 1 MHz to test the performance of the macPSi sensor in the absence and presence of organic and pesticide molecules. The inductance of the fabricated external air coil is an 18 turn, 30 µH, and with a cross-sectional area of about 80 cm². The coil was made from a 3mm diameter copper wire to ensure very low resistance. The AC voltage was fixed at 10 mV, and the circuit was connected in series form. Different low concentrations of organic solvents and pesticides (0.1, 0.5, 1, 1.5, and 2 ppm) were exposed separately to the sensor to confirm the optimized electrode configuration are illustrated in Fig. 3.
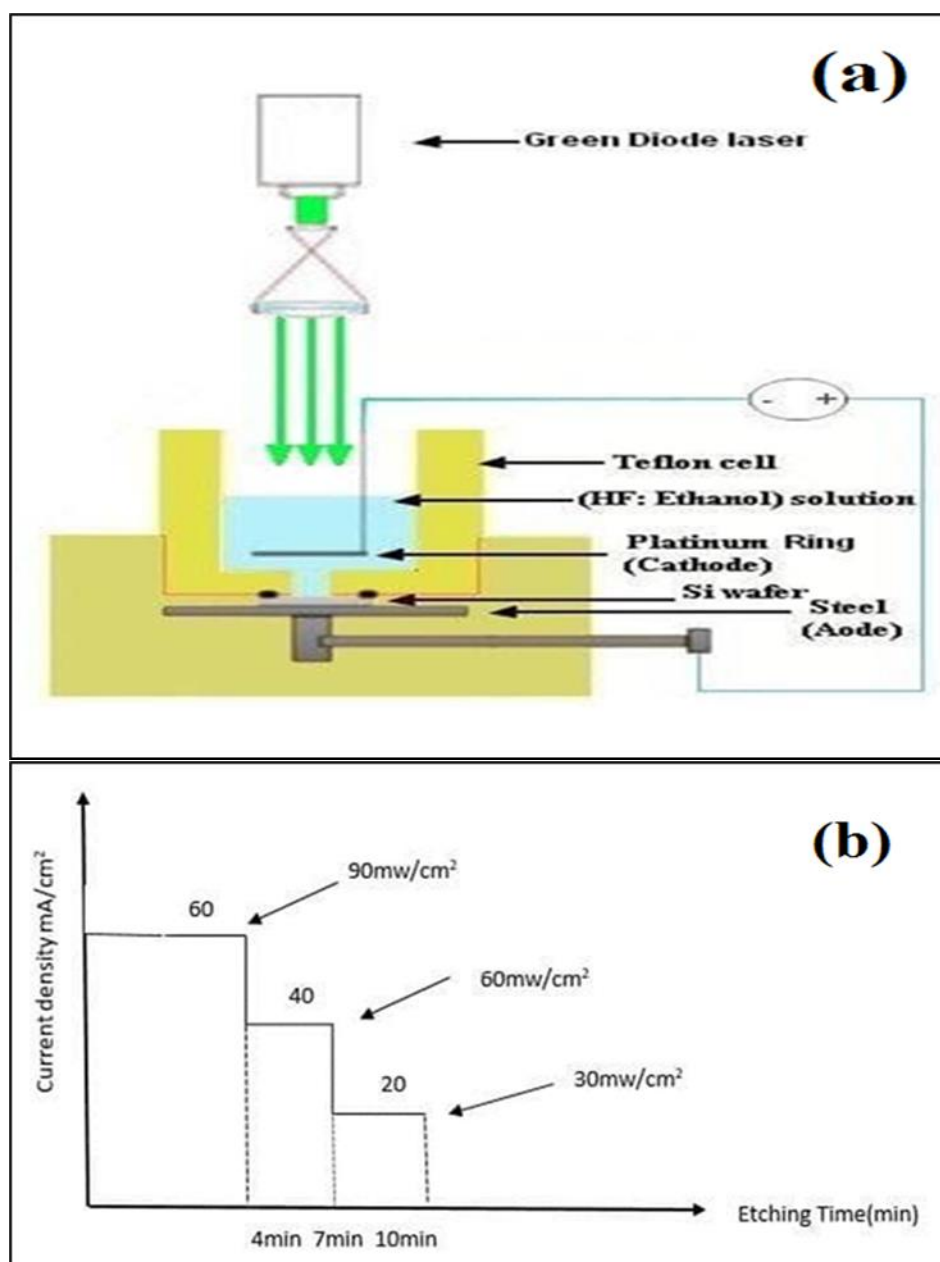

Figure 1: (a) schematic representation of photoelectrical etching, (b) graded laser irradiation process.
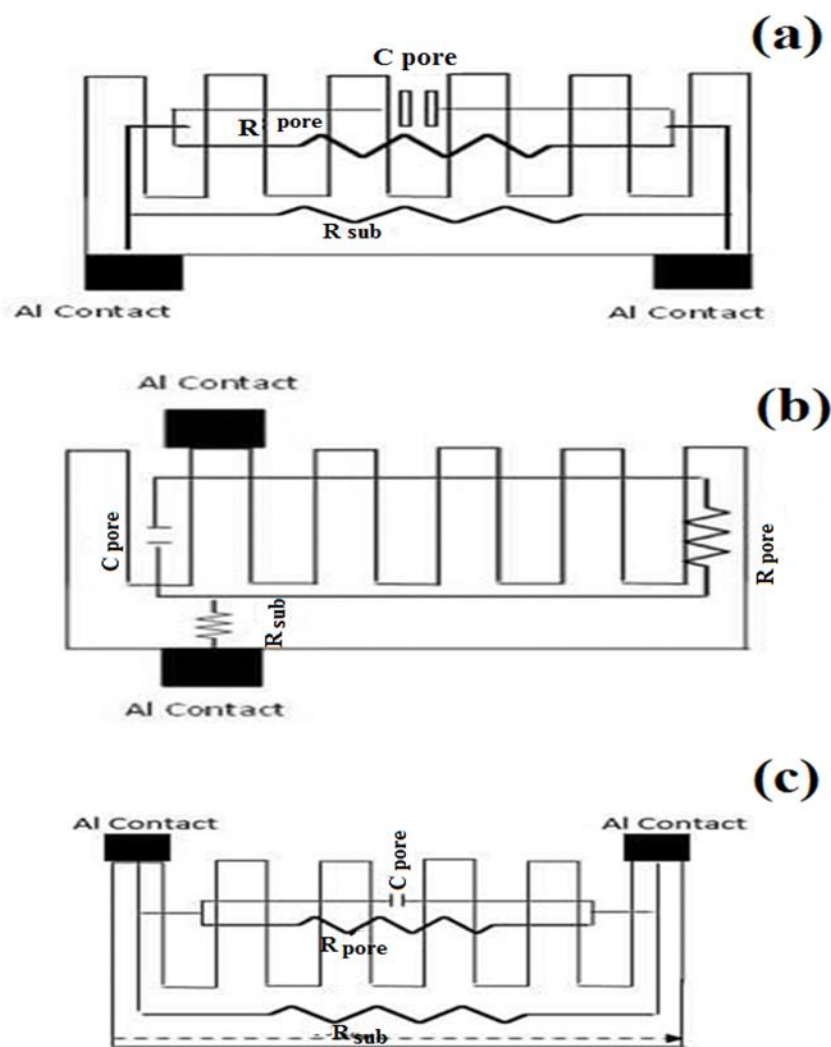
Figure 2: A schematic representation of coplanar AL electrodes configurations for (a) backside (S1), (b) front-back (S2) and (c) front side (S3) on the macPSi layer [20].
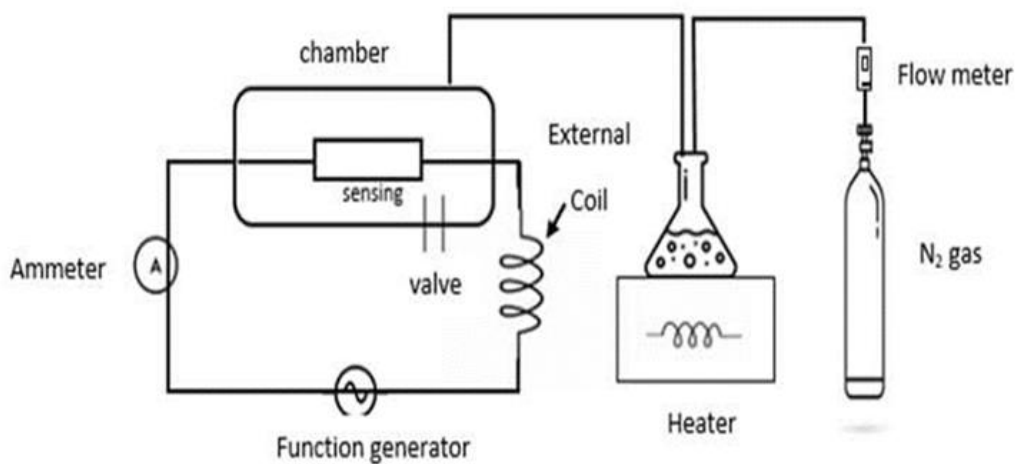
Figure 3: A schematic representation of organic and pesticide sensing measurements set – up.

3. Results and Discussion

3.1. Characterization of Double-layer macPSi

The porosity and the layer thickness of the macPSi layer are (~71%) and (~6.8 μm), respectively. These values were computed from gravimetric measurements [22]. The Si etching pathway was accomplished in three steps via laser power densities of 90, 60, and 30mW/cm^2. The morphological aspects of the macPSi etched by the above three levels of power density were investigated by SEM micro-image analysis. The surface morphology of the double macPSi layer is composed of a complex network of pores, mud, and trenches with different sizes dimensions, and forms. As depicted in Fig. 4a and b for macPSi, there are two morphologies: "upper layer" is the mud-like morphology of non-connected trenches of various dimensions, and the "lower layer" is the pore-like morphology of various pore dimensions; synthesized outside and among the mud-like structures Fig. 4a. Fig. 4b illustrates pores and trenches dimensions of (0.83-1.31) μm for pores and trenches of (1.5-5.3) μm. The formation of these specific morphologies could have resulted from the graded reduction of irradiation laser power density and etching current density during the etching pathway. This process may modify the Si dissolution route during the pore creation and leads to the formation of a complex porous network with various morphologies. Inside, each morphology, the pores, and muds are aligned in random directions. The formation mechanism behind these results can be understood from the Steven E. model [23], in which the etching manner depends on the rate of photo-generated electron-hole couples. This rate is modified when reducing the irradiation laser power density. The etching photocurrent I$_{ph}$ was induced as a result of the photo-generated electron-hole couples are given by Eq. (3) [24].

$$I_{ph} = (1 - R_{PSi}) \times Pin \times \eta \times q_e / h\upsilon \tag{3}$$
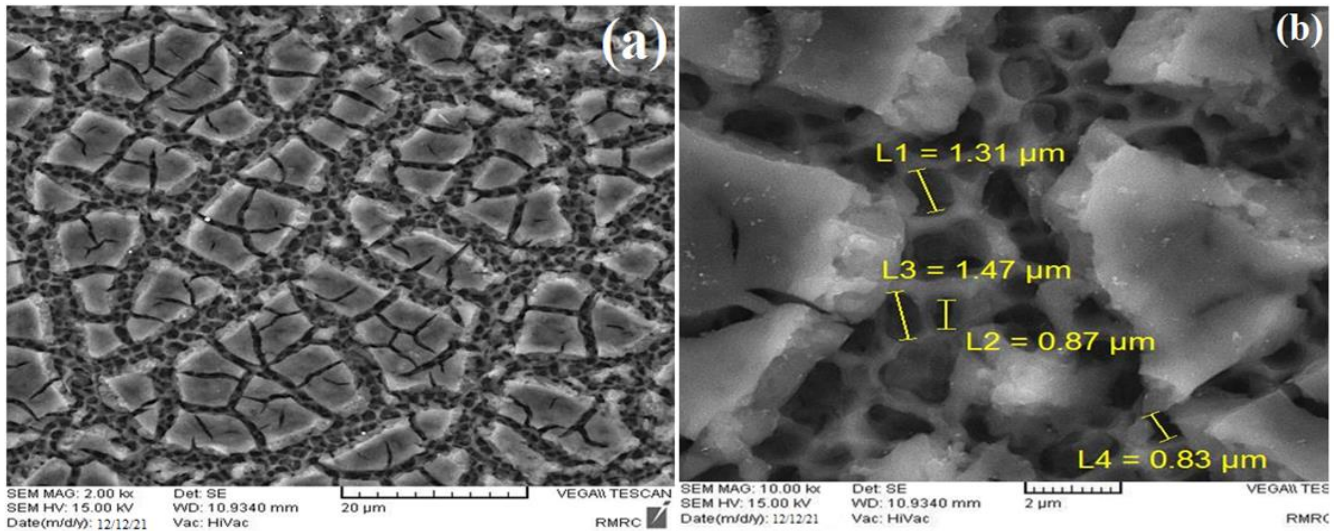

Figure 4: (a) SEM micro-image of macPSi substrate, and (b) magnified micro-image.

Where Pin refers to the incident laser power, R$_{PSi}$ is the reflectivity of the porous matrix, η is quantum efficiency, υ is a laser frequency, h is the Blank constant and qe is the electron charge. Based on this equation, reducing the laser power can modify the etching current and hence the silicon dissolution process. The dependence of pores dimension on etching current density (J) during the graded etching pathway is given in Eq. (4) [25].

$$D = \sqrt{\frac{4J}{\pi C c^{\frac{3}{2}} N}} \exp\left(\frac{Ea}{KT}\right) \tag{4}$$

Where; (D) is the mean diameter of pores, (C) is the HF concentration, E$_a$ =345 meV, C=3300, and N is the density of pores at the surface. The form of silicon species (pores, muds, and trenches) is therefore a fingerprint of current density. Any variation of current density which results from laser power density will modify the surface morphology of the porous layer.

The photoluminescence spectrum of the macPSi layer is illustrated in Fig. 5. It shows two distinguishable peaks of the macPSi layer with emission wavelengths 530and 651 nm corresponding to two energy gaps: 2.4 eV and 1.92 eV, respectively. The presence of double PL peaks is a specific feature of the existence of double morphology (muds and pores-like structures) with two silicon nanocrystallites size distributions. This explanation is in very good agreement with the quantum confinement model of electrically charged carriers within the matrix of the macPSi layer. The PL intensity is strongly related to the amount of Silicon nanocrystallites within the matrix whereas; the peak emission wavelength is related to the dimensions of the Si nanocrystallites [26-28].
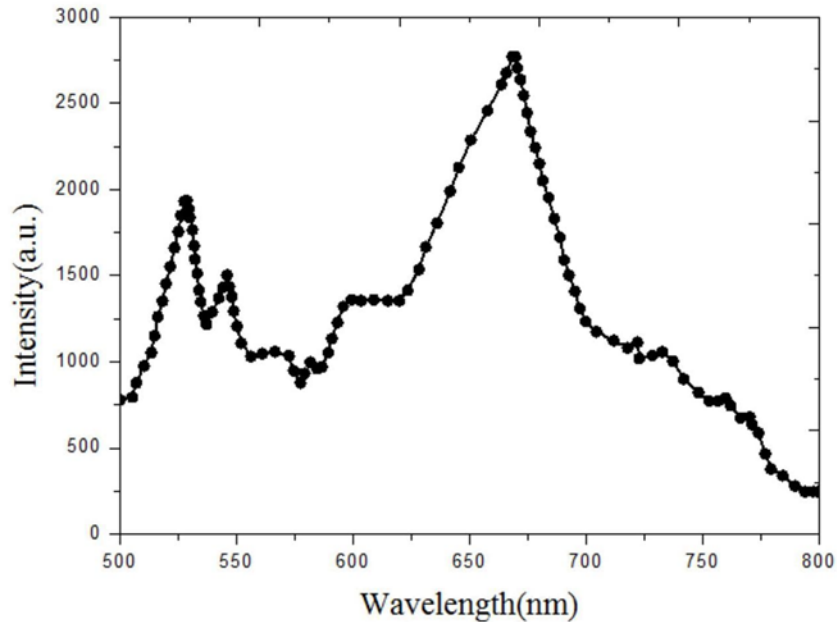

Figure 5: PL spectrum of the macPSi layer.

The structural property of the synthesized porous layer is shown in Fig. 6, which displays the XRD spectrum of the double macPSi layer. The double morphology structure is still in the crystalline (100) phase planes with 2θ of about 32.8°.
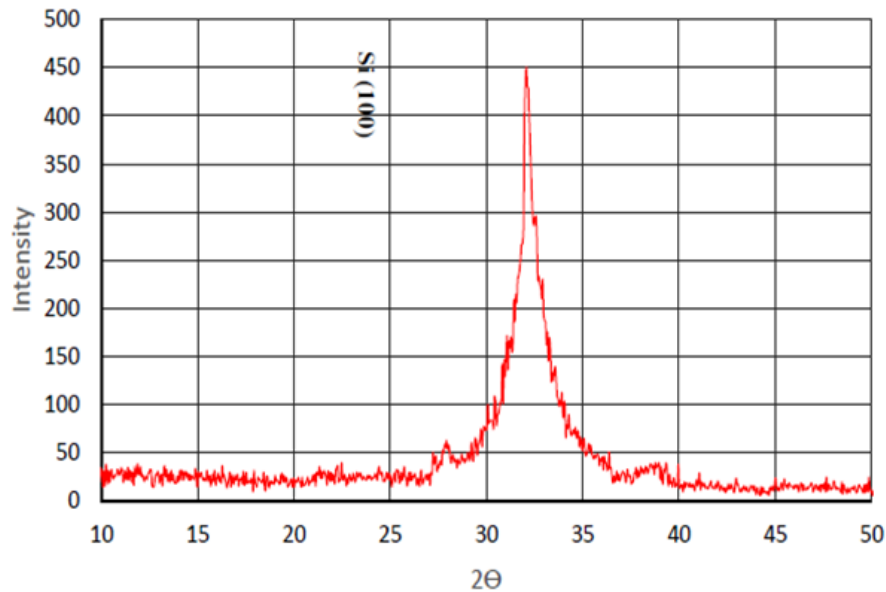

Figure 6: XRD diffraction pattern of the macPSi layer.

3.2. Double-layer macPSi Sensor for Sensing Organic Vapors

The sensing principle of the macPSi sensor depends on monitoring the variations in the dielectric constant inside the macPSi layer and hence, the resonance frequency after inserting the tested chemical molecules in porous matrix pores. The three various types of the synthesized macPSi sensors, (S1), (S2), and (S3) on the macPSi layer, were inspected with the most common organic solvents for chlorpyrifos (methanol and acetone), and their activity was compared to reach the best electrode configuration for sensing pesticide named 'chlorpyrifos'. The easiest, low-cost, and most effective technique for testing chemical sensors is when using a simple electrical circuit; based on the concepts of impedance matching between the macPSi capacitive sensor and appropriate external coil [29]. According to this technique, any tiny variation in the chemical interaction between target molecules and the surface of the material could be highly detected and converted to an electrical signal. Dependent on the resonance frequency shift, this simple technique is used to detect the low concentration of organic vapors and pesticides. Fig. 7 demonstrates the current as a function of the frequency of AC applied voltage for various sensors: S1, S2, and S3. At the resonance frequency, the current in the impedance matching circuit reaches a peak value. In this figure, when the sample is tested in the absence of gas at room temperature, the resonance frequencies obtained are around (370,490, and 392 KHz corresponding to the highest values of current (91, 83 and, 98 mA) for S1, S2, and S3, respectively. The lowest value of methanol and acetone vapors concentration (0.1 ppm) was exposed to the sensor at room temperature. An ultra-response was achieved; in the form of a shift in the resonance frequency to a higher frequency. The shift obtained with methanol was higher than that of acetone. For the S1, S2, and S3 sensors, the new values of resonance frequency for methanol and acetone are (424 and 468 KHZ), (523 and 580 KHZ), and (473 and 510 KHz) respectively. The corresponding maximum currents at resonance are: (104 and 116 mA), (146 and 165 mA), and (107 and 124 mA), respectively. The different configurations between methanol and acetone provide us with a novel approach to separate a binary methanol−acetone mixture. Methanol has a typically polar hydroxyl group and a methyl group, whereas acetone has a carbonyl group and two methyl groups. The studied materials with strong electron-donating or electron-accepting functional groups and relative larger accessible surface area (i.e) exhibit a strong methanol adsorption capacity, and thus have a significant selectivity toward methanol in Fig. 7, the current with methanol is greater than that of acetone and the current increase after exposure to organic vapors is strongly related to the effective dielectric constant of porous silicon as expressed in Eq. (5) [30].
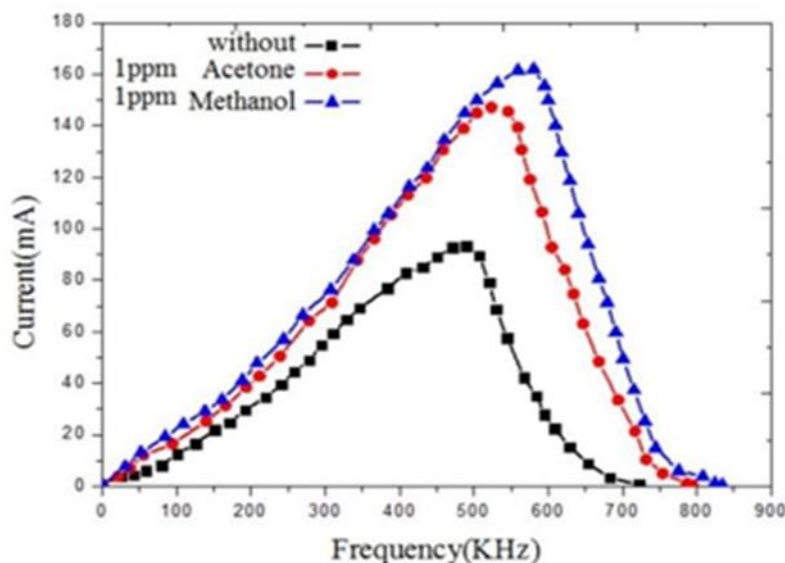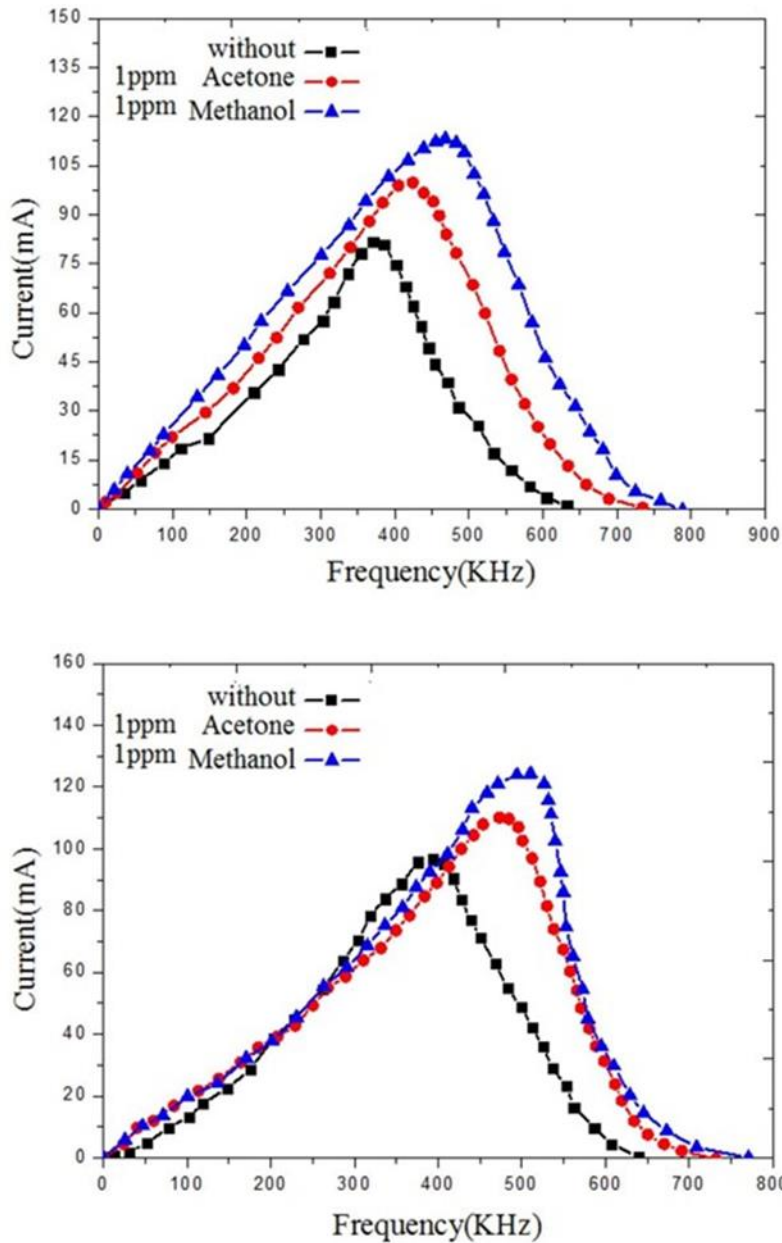
Figure 7: Current-Frequency properties of impedance matching circuit of organic vapors, (a) S1, (b) S2, and (3) S3 sensors at (0.1 ppm) concentration of methanol and acetone.

$$J_{PSi} = \varepsilon_{rpsi}\varepsilon_o\, \mu eff\, V^2/d^3 \qquad (5)$$

Where ε_{rpsi} is a dielectric constant of PSi, ε_o dielectric constant of air, μeff is the mobility of the charge carriers, V is the applied voltage and d is the porous layer thickness. As a result of loading targets molecules within the double morphology layer, the effective dielectric constant of the macPSi layer is modified and is given in Eq. (6) [31].

$$\varepsilon_{rpsi} = \varepsilon_{rsi-p}(\varepsilon_{rsi} - \varepsilon_{r\, pore}) \qquad (6)$$

Where ε_{rpsi}, is the effective dielectric constant of the porous matrix, $\varepsilon_{r\, pore}$, and ε_r Si are the dielectric constant of filling pores that targets molecules (methanol or acetone) and Si, respectively. Since the dielectric constant of methanol (34) is higher than that of acetone (22.5), the ε_{rpsi} in the presence of methanol is higher than that of acetone and the current increases with increasing ε_{rpsi}.

Fig. 8 clearly shows that the resonance frequency for all sensors increases linearly with the concentration of methanol and acetone, with a resonance frequency in methanol higher than in acetone. This is because a higher concentration increases the possibility of the interaction between the sensor and the target molecules. This in a way will modify the ε_{rpsi} efficiently. Moreover, at the fixed type of organic vapors, the performance of the fabricated sensors varies with the electrode configuration. The higher response was achieved with S3 of about 103.13 KHz/ppm and 84.5 KHz/ppm, while for S2 the response was 79.76 KHz/ppm and 54.1 KHz/ppm sensor. Finally, the lowest response was seen with S1 which gave 74.69 KHz/ppm and 56.28 KHz/ppm for methanol and acetone, respectively. For Ohmic contact metallization, the measured capacitance of the sensor is the series combination of porous silicon matrix C_{PSi} and junction capacitance C_j between the macPSi layer and bulk silicon. The insertion of target molecules within the C_{PSi} leads to an increase in the capacitance which will decrease the sensor capacitance; hence pushing up the resonance frequency to higher values as compared with the air-filled matrix. The high sensitivity arises from a higher surface area and the double morphology structures on the surface are so efficient to adsorb a large number of target molecules. The high sensitivity of the sensor towards ultra-low methanol concentration as compared with acetone is strongly related to the dielectric constant. The high response achieved with the S3 sensor may be due to its high capacitance value and the effective exposure area; since higher capacitance increases the response of the sensor. The measured experimental values of the macPSi sensor with an air-filled matrix for S1, S2, and S3 are 1.6 nF, 1.4 nF/μm^2, and 2.6 nF, correspondingly. The sensor's capacitance varies with the dielectric constant of the sensing target molecules within the double morphology layer and the electrode configuration. Besides, the substrate's resistance RSub hardly affects the sensor's sensitivity; because of the wafers high doping density of donor impurities in the wafer. The total sensor's impedance doesn't only vary with the relative permittivity of the sensing target molecules but also with the separation between the electrode and the resistance of the Ohmic contact. Therefore; the variation in the sensor's capacitance is mainly contributed by the relative permittivity value within the porous matrix. When the target molecules are integrated, a noticeable change is observed in the capacitance and hence; a shifting in resonance frequency is recorded. To explore the aging effects on the performance of fabricated sensors for long-term operation, the frequency shift was measured repeatedly; every five days during the 40 days at a fixed (0.1ppm) concentration of methanol. The test displayed a highly stable performance of macPSi sensors, as shown in Fig. 9.
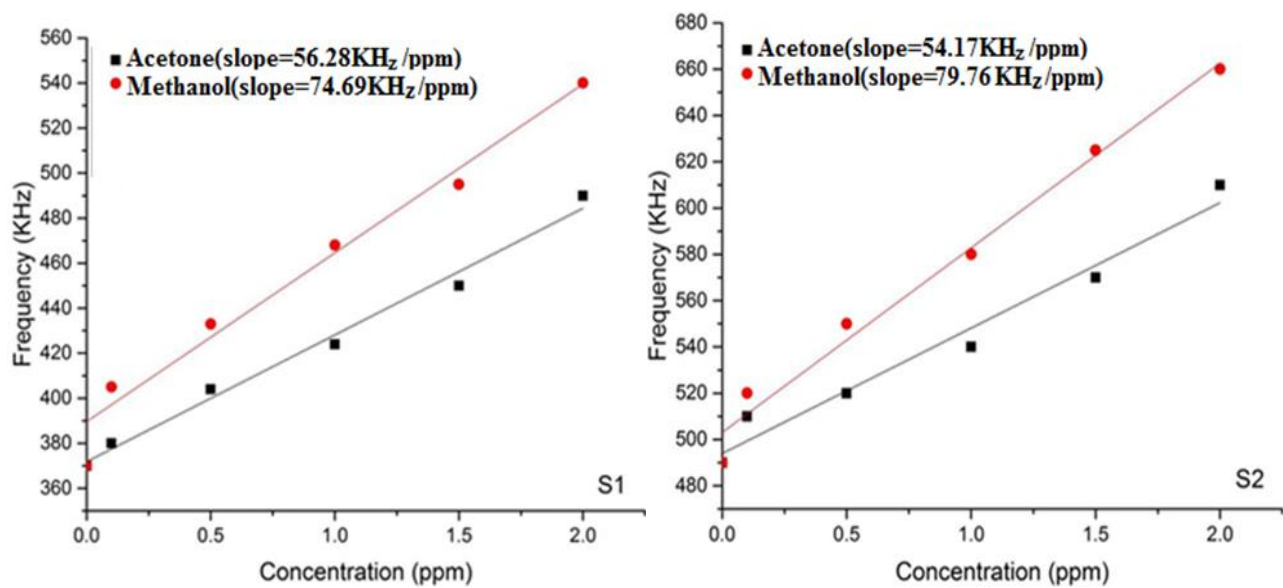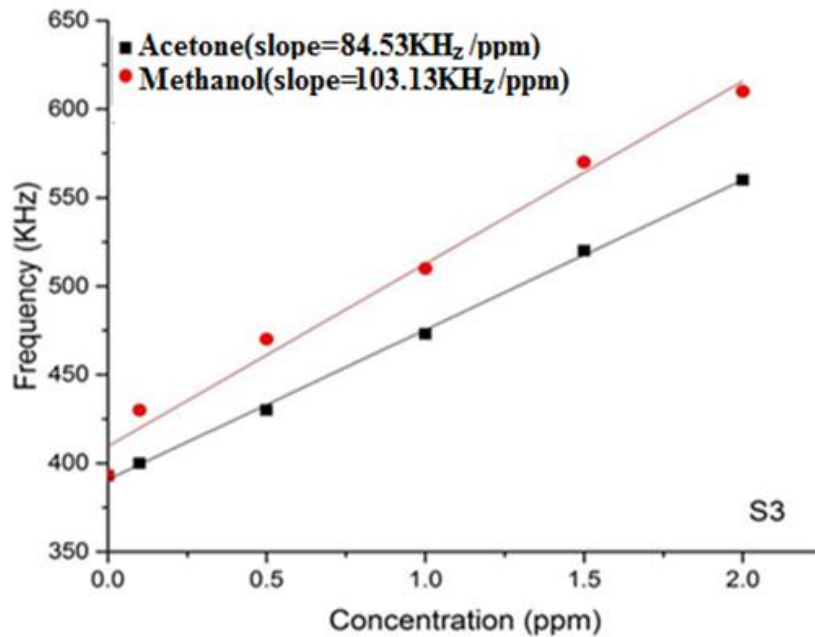
Figure 8: Dependence of resonant frequency (f) on methanol and acetone concentrations (0.1ppm to 2ppm) for S1, S2, and S3 sensors.
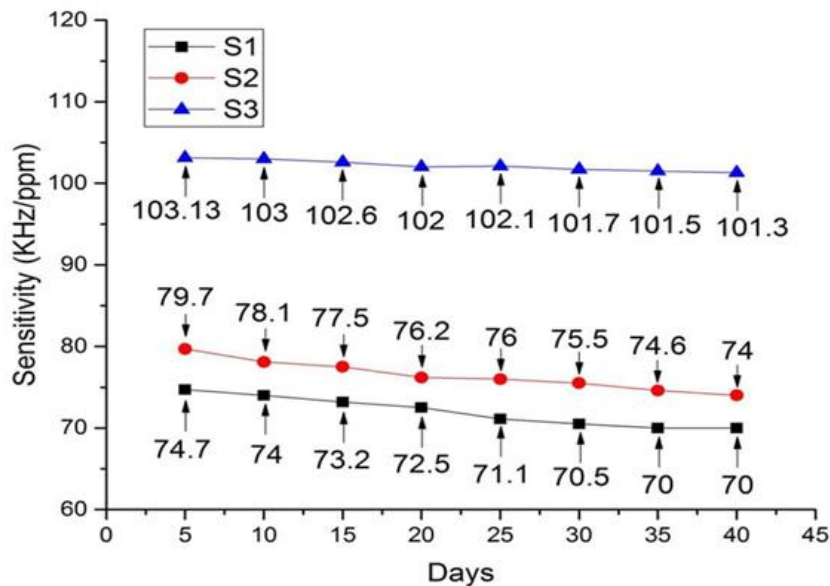

Figure 9: A dropping frequency shift of all S1, S2, and S3 sensors at a time for various reduction rates (0.063%, 0.07%, and 0.017).

As the natural oxidation rate increases, the reduction rate insensitivity increases. Thus, the S3 sensor offers excellent stability due to its lower reduction rate which is strongly related to the effective exposure volume (pores and trenches) to the ambient atmosphere. Based on sensitivity and stability results, S3 sensor is the best to adopt for pesticide sensing.

3.3. Double-layer macPSi Sensors for Detection of Pesticide Concentration in Organic Solvents

The ultra-low concentration of Chlorpyrifos solutions was prepared by dissolving a specific weight of Chlorpyrifos in 100 ml of methanol and then is diluted to obtain 0.1, 0.5, 1, 1.5, and 2ppm. The Chlorpyrifos was loaded into

the S3 sensor and the shift of resonance frequency Δf was measured for each concentration. After each measurement, the sensor was cleaned with de-ionized water and dried using nitrogen gas. The macPSi sensor's response depends essentially on the dielectric constant of the Chlorpyrifos solution (concentration of Chlorpyrifos) and the possibility of filling the macPSi matrix. The concentration of Chlorpyrifos in the solution is calculated by measuring the Δf of the sensor, and the possibility of filling the macPSi layer is tested via the repetition of measured values. Fig. 10 presents the dependence of the resonant frequency (f) on Chlorpyrifos concentrations (0.1ppm to 2ppm) for the S3 sensor. It is easy to notice in this figure that the resonance frequency increases linearly with the concentration of Chlorpyrifos, and the value of resonance frequency in methanol is higher than that of acetone. The sensitivities of S3 were 129.9 KHz/ppm and 105.3 KHz /ppm for Chlorpyrifos in methanol and acetone, respectively. The sensitivity curve, which represents the relation between the frequencies shift Δf and the Chlorpyrifos concentrations are shown in Fig. 11. In this figure, the concentrations of Chlorpyrifos in methanol and acetone varied from 0.1 to 2 ppm, and the frequency shift linearly increases in the regime of tested concentration. In this figure, each experimental data was the mean value of five independent measurements. The slope of the linear part of the curve represents the sensitivity of the sensor. The detection limit (LOD) was computed and 0.004 and 0.09 ppm for chlorpyrifos in methanol and acetone, respectively. Remarkably, the use of macPSi in the sensing process with impedance matching circuit made significant contributions in detecting pesticides compared to published work elsewhere [32]. The Obtained LOD of the macPSi sensor is lower than that measured by an optical method that employs the SERS technique. The current sensor represents a potential possibility for enhanced sensitivity, linear performance, and low-cost design solutions. Where, Acceptable Daily Intakes (ADI) for Chlor- pyrifos as 0.01 mg/kg.
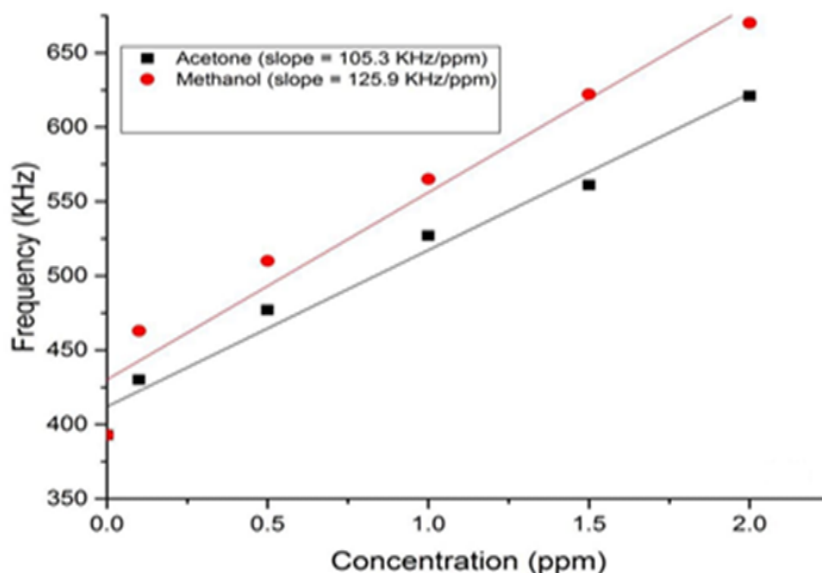

Figure 10: Resonant frequency (f) dependence on Chlorpyrifos concentrations (0.1ppm to 2ppm) for the S3 sensor.
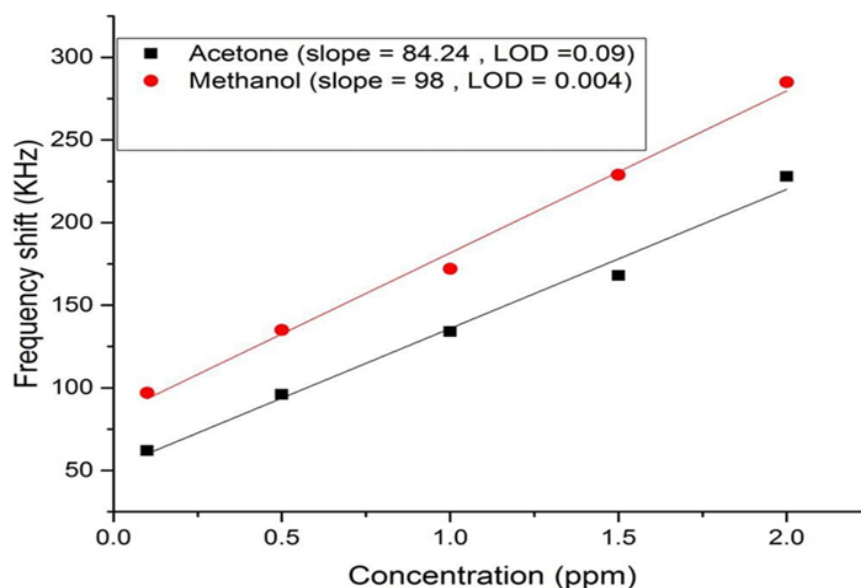
Figure 11: Relation between the frequency shift Δf and the Chlorpyrifos concentration (0.1 to 2 ppm) in methanol and acetone.

4. Conclusions

In this work, highly sensitive impedance matching chemical sensors were efficiently fabricated for detecting ultra-low organic vapors and pesticide concentrations. The based Double morphology macPSi layer was fabricated by photo electrochemical process with graded laser irradiation power density for different periods. Three various types of chemical sensors configurations: coplanar back electrode, front-back electrode, and the coplanar front electrode on the macPSi were synthesized and tested. The coplanar top electrode configuration was found the best in terms of higher sensitivity and stability. The impedance matching sensor is capable of detecting ultra-low concentrations of Chlorpyrifos pesticide with excellent LOD of about 0.004 and 0.09 ppm in methanol and acetone, respectively. The double-layer macPSi can be employed as a potential choice for developing an efficient, low-cost, and simple operation sensor for the quantitative detection of chemicals.

Conflict of Interest

The authors declare that they have no conflict of interest.

References

[1] H. Yong, S. Xiao, T. Dong, and N. Pengcheng, "Gold Nanoparticles with Different Particle Sizes for the Quantitative Determination of Chlorpyrifos Residues in Soil by SERS," *International Journal of Molecular Sciences*, vol. 20(11): 2817, 2019.

[2] L.A.Wali, K.K. Hasan, and A. M. Alwan, "Rapid and highly efficient detection of ultra-low concentration of penicillin G by gold nanoparticles/porous silicon SERS active substrate," *Spectrochimica Acta Part A: Molecular and Biomolecular Spectroscopy 206, 31-36*,vol.206: p.31–36, 2019.

[3] B. S Larsen , P. Stchur, B. Szostek, *et al*., "Method development for the determination of residual fluorotelomer raw materials and perflurooctanoate in fluorotelomer-based products by gas chromatography and liquid chromatography mass spectrometry,*" Journal of Chromatography A*,vol.31;1110(1-2),p.117-24, 2006.

[4] A. M. Alwan, D. A. Hashim, and M. F. Jawad, "Optimizing of porous silicon alloying process with bimetallic nanoparticles." *Gold Bulletin* vol.51, no. 4, p. 175-184, 2018.

[5] W. H Ali, A. B. Dheyab, A. M. Alwan, and Z. S. Abber, "Study the role of mud-like Psi morphologies on the performance of AuNPS SERS sensor for efficient detection of amoxicillin," *AIP Conference Proceedings*, vol. 2290, p.050061, 2020.

[6] P. Rodríguez, Ovidio, and U. Pal, "Enhanced plasmonic behavior of bimetallic (Ag-Au) multilayered spheres," *Nanoscale research letters,* vol. 6, no. 1, p. 279, 2011.

[7] D. A. Hashim, A. M. Alwan, and M. F. Jawad, "An investigation of Structural Properties of Monometallic (Ag, Pd) and Bimetallic (Ag@ Pd) Nanoparticles Growth on Macro Porous Silicon," *International Journal of Nanoelectronics & Materials*, vol.11, no. 4, 2018.

[8] A. M. Alwan, A. B. Dheyab, and A. J. Allaa, "Study of the influence of incorporation of gold nanoparticles on the modified porous silicon sensor for petroleum gas detection," *Engineering and Technology Journal*,vol. 35, no. 8 Part (A) Engineering ,p. 811-815, 2017.

[9] C. Zhai, Y.Li, Y. Peng and T. Xu "Detection of chlorpyrifos in apples using gold nanoparticles based on surface enhanced Raman spectroscopy," *International Journal of Agricultural and Biological Engineering*, vol. 8, p.113-120, 2015.

[10] A. M. Alwan , R. A. Abbas, and A. B. Dheyab, "Study the characteristic of planer and sandwich PSi gas sensor (Comparative Study)," *Silicon*, vol.10, no. 6, p. 2527-2534, 2018.

[11] L. A. Wali, Layla, A. M. Alwan, A. B. Dheyab, and D. A. Hashim,"Excellent fabrication of Pd-Ag NPs/PSi photocatalyst based on bimetallic nanoparticles for improving methylene blue photocatalytic degradation," *Optik* ,vol.179, p.708-717, 2019.

[12] M. H. Kareem, M. Adi, and H. T. Hussein, "The Effect of Current Density on the Properties of Porous Silicon Gas Sensor for Ethanol and Methanol Vapour Detection," *Journal of Applied Sciences and Nanotechnology*, vol. 1, Issue 4, PP. 52-60, 2021.

[13] A. M. Alwan, I. A. Naseef, and A. B. Dheyab, "Well controlling of plasmonic features of gold nanoparticles on macro porous silicon substrate by HF acid concentration," *Plasmonics,* vol. 13, no. 6, p. 2037- 2045, 2018.

[14] F. Giorgis, E. Descrovi, A. Chiodoni, E. Froner, *et al*., "Porous silicon as efficient surface-enhanced Raman scattering (SERS) substrate,"*Applied Surface Science*, vol. 254, p.7494–7497, 2008.

[15] A. M. Alwan, A. J Hayder, A. A Jabbar, "Study on morphological and structural properties of silver plating on laser etched silicon," *Surface and Coatings Technology*, Vol. 283, 15, p. 22-28, 2015.

[16] G. Foti,E. Rimini,S. U. Campisano, "Laser annealing of Pb-implanted silicon," *physica status solidi (a),*vol. 47 no.533,1978.

[17] A. B. Dheyab, A. M. Alwan, M. Q. Zayer, "Optimizing of gold nanoparticles on porous silicon morphologies for a sensitive carbon monoxide gas sensor device," *Plasmonics,* vol. 14(2), p.501–509, 2019.

[18] G. R. Stevenson, J. G. Concepcion, *et al*.,"Electron spin resonance study of nitrosamine anion radicals,"*The Journal of Physical Chemistry*, vol.77 (5), p.611-4, 1973.

[19] M. Q., Alwan M., A. S. and A. B. Dheyab, "Accurate controlled deposition of silver nanoparticles on porous silicon by drifted ions in electrolytic solution," *Current Applied Physics,* vol.19, p.1024-1030, 2019.

[20] A. M. Alwan and A. B. Dheyab,"Room temperature CO2 gas sensors of AuNPs/mesoPSi hybrid structures," *Applied Nanoscience*, vol. 7, p.335–341, 2017.

[21] Y. Liu, Y. Zhang, H. Wang, and B.Ye, "Detection of pesticides on navel orange skin by surface-enhanced Raman spectroscopy coupled with Ag nanostructures," *International Journal of Agricultural and Biological Engineering*, vol. 9(2), p.179－185, 2016.

[22] J. Li, Q.Wang, J. Wang, M. Li, X. Zhang, L. Luan, P. Li, W. Xu, "Quantitative SERS sensor based on self-assembled Au@Ag heterogeneous nanocuboids monolayer with high enhancement factor for practical quantitative detection," *Analytical and Bioanalytical Chemistry*, vol.413 (16), p.4207-4215, 2021.

[23] E. J.Steven, N.M.S. Sirimuthu, "Quantitative surface-enhanced Raman spectroscopy," Chemical Society Reviews journal, vol. 37(5), p.1012–24, 2008.

[24] X. Cao, S. Hong, Z. Jiang, Y. She, S.Wang, C. Zhang, *et al.,* "SERS-active metal-organic frameworks with embedded gold nanoparticles," *Analyst* vol.142, p. 2640–2647, 2017.

[25] D. I. Nathan, H. Cynthia, and V. Elizabeth,"Nanoparticle Properties and Synthesis Effects on Surface-Enhanced Raman Scattering Enhancement Factor: An Introduction," *Scientific World Journal*, Article ID 124582, p.12, 2015.

[26] A. A. Salman, F. I. Sultan, U. M. Nayef, "Structural, Chemical and Morphological of Porous Silicon Produced by Electrochemical Etching," *Engineering and Technology Journal*, vol. 30, no. 5, P. 855-867, 2012.

[27] D. S Jubair, A. M Alwan, W. K. Hamoudi, "Sensing Performance of Mono and Bimetallic Nano Photonics Surface Enhanced Raman Scattering (SERS) Devices,"*Engineering and Technology Journal*, vol. 39, no. 7, P. 1174-1184, 2021.

[28] N. J.Zahid, B. Hashime, M. J. Rasib, A. Mohtfir, "Synthesis and optimization of silver nanoparticles-antibody Herceptin conjugation for surface-enhanced Raman scattering (SERS)," *Engineering and Technology Journal*, vol.33, no. 9, p.1655-1662, 2015.

[29] H. Lin, J. Mock, D. Smith, T. Gao, M.J. Sailor, "Surface-enhanced Raman scatteringfrom silver-plated porous silicon," *Journal of Physical Chemistry B*, vol. 108 (31), p.11654–11659, 2004.

[30] A. Yu. Panarin, V.S. Chirvony, K.I. Kholostov, P.-Y. Turpin, S.N. Terekhov, "Formation of SERS-active silver structures on the surface of mesoporous silicon," *Journal of Applied Spectroscopy*, vol.76 (2), p. 280, 2009.

[31] M. B. Gongalsky, U.A.Tsurikova, J.V.Samsonova, G.Z.Gvindzhiliiia, *et al.*, "Double etched porous silicon nanowire arrays for impedance sensing of influenza viruses," *Results in Materials*, vol. 6, p. 100084, 2020.

[32] S. Feng, H. Yaxi, M.Luyao, X. Lu, "Development of molecularly imprinted polymers-surface-enhanced Raman spectroscopy/colorimetric dual sensor for determination of chlorpyrifos in apple juice," *Sensors and Actuators B: Chemical*, vol. 241, p. 750-757, 2017.